Surface Freezing on Patterned Substrates

Martin Heni and Hartmut Löwen

Institut für Theoretische Physik II, Heinrich-Heine-Universität Düsseldorf, Universitätsstrasse 1, 40225 Düsseldorf, Germany

(Received 5 June 2000)

We show that the structure of a substrate pattern drastically influences the nature of surface freezing. By using phenomenological theory and computer simulations of a hard sphere fluid next to a substrate formed by a periodic array of fixed spheres, we find that a pattern which is commensurate with the bulk crystal induces complete surface freezing through a cascade of layering transitions. A rhombic pattern, on the other hand, either generates a crystalline sheet which is unstable as a bulk phase or prohibits surface freezing completely.

PACS numbers: 68.35.Rh, 64.70.Dv, 82.70.Dd

While bulk phase transitions are by now well understood, the presence of a surface induces a much richer scenario of interfacial phase transitions such as wetting [1,2] or surface reconstruction [3] which is interesting from a fundamental point of view and important for many technical applications. Surface freezing is a peculiar type of wetting transition, where a liquid surface builds up spontaneously several crystalline layers at temperatures well above bulk freezing. Unlike spherical particles, chain molecules such as alkanes [4] and alcohols [5] may form a crystalline sheet on top of their free liquid-vapor interface. The corresponding molecular understanding has greatly advanced via both phenomenological theories [6] and computer simulations [7].

In contrast to a free surface, spherical particles may exhibit surface freezing near a patterned substrate. In fact, well-characterized substrates with periodic nanosized chemical and topographic structures can now be prepared using such techniques as lithographic procedures. Used as a template, a patterned substrate can profoundly influence the nature of wetting transitions, as recently demonstrated for chemically heterogeneous surfaces [8,9].

In this Letter we investigate how surface freezing is influenced and controlled by an underlying topographically patterned substrate. We focus on a fluid of spherical particles modeled as hard spheres in the neighborhood of a substrate composed of fixed hard spheres forming a periodic two-dimensional array. There are two main reasons for our approach. First, the model is kept simple since the thermodynamics and phase diagram of the bulk hard sphere system depend only on the volume fraction η. The bulk hard sphere systems exhibit a freezing transition with volume fractions $\eta_f = 0.494$ and $\eta_s = 0.545$ of the coexisting fluid and solid [10]. Understanding the molecular principles of surface freezing is thus possible within this "minimal" framework. Second, our model is actually applicable for index-matched sterically stabilized colloidal suspensions on periodic patterned substrates which can be prepared by "gluing" colloidal spheres onto a periodic pattern [11]. Such colloidal model systems bear the further advantage that real-space experiments can be performed, as the relevant length scale is shifted from the microscopic to the mesoscopic regime. Nevertheless our model may also serve as a simple microscopic description of molecular systems such as liquid metals on crystalline surfaces. Consequently, all of our predictions can, in principle, be verified in real-space experiments of colloidal suspensions [11] or by scattering techniques probing the inhomogeneous microscopic structure of liquid metals near crystalline substrates [12].

As a result, we show that a pattern which is commensurate with the bulk crystal induces complete surface freezing with an onset far away from bulk coexistence. This proceeds via a cascade of subsequent layering transitions as the bulk freezing transition is approached. On the other hand, a surface pattern which is distorted from the compatible one leads either to incomplete surface freezing or completely prevents surface freezing. For small distortions there is incomplete wetting by crystalline layers which are unstable as a bulk phase. These layers directly inherit their structure from the underlying pattern. However, above a critical distortion surface freezing does not occur anymore.

Our results are based on computer simulations and phenomenological theory. Monte Carlo simulations were performed for N hard spheres with diameter σ at temperature T in a rectangular box of size $V = L_x L_y L_z$ with periodic boundary conditions in x and y directions and two patterned walls at distance L_z confining the system perpendicular to the z direction. Both constant volume (NVT) and constant wall-pressure (NPT) ensembles were used and it was carefully checked that the simulation results were ensemble independent. Finite size effects were systematically studied by varying the box lengths and areas from $L_x L_y = 16\sigma^2$ to $L_x L_y = 271\sigma^2$ and $L_z = 40\sigma$ to $L_z = 100\sigma$, corresponding to particle numbers between $N = 640$ and $N = 10\,400$. The substrate pattern consists of hard spheres with the same diameter σ as the mobile ones. These spheres were fixed in a plane on a two-dimensional lattice which was compatible with the lateral periodicity of the simulation box. Both a triangular pattern, resulting from a (111) surface of the face-centered-cubic (fcc) bulk crystal coexisting with the fluid, and a distorted rhombic pattern were used (see Fig. 1). In the triangular case, the lattice constant $a_\triangle$ is 1.1075σ

 0031-9007/00/85(17)/3668(4)$15.00

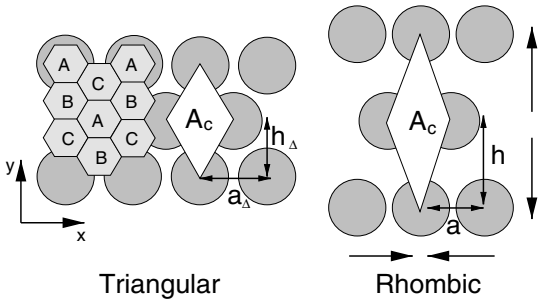

FIG. 1. Geometry of the triangular and rhombic substrate pattern. The rhombic pattern results from the triangular one by distorting the lattice, as indicated by the arrows, such that the area A_c of the unit cell remains constant. For the triangular pattern the three types A, B, and C of honeycomb cells defining the stacking order parameter are also shown.

with a height $h_\triangle$ of the equilateral triangle of $\sqrt{3}\,a_\triangle/2$. The rhombic pattern has a lattice constant a smaller than $a_\triangle$ but a larger height h, such that the area $A_c = ah$ of the elementary cell remains unchanged (see Fig. 1). We characterize the rhombic distortion via the lateral strain $\epsilon = \sqrt{[(a - a_\triangle)/a_\triangle]^2 + [(h - h_\triangle)/h_\triangle]^2}$. Obviously, ϵ vanishes for a triangular pattern, but for a pattern not compatible with the bulk solid we have $\epsilon > 0$. Since all interactions are of excluded-volume type, the thermal energy k_BT scales out and the system is completely described by the reduced bulk pressure $P^* = P\sigma^3/k_BT$ and the lateral strain ϵ.

During our simulations we monitored a suitable order parameter Ψ_n, which probes the ideality of stacking in the nth layer and is sensitive to layerwise surface freezing. In what follows, we explain its definition for a triangular pattern, the generalization to a rhombic pattern being straightforward. The position of the minima in the laterally integrated density profile was used to define the spacing of the nth layers in the z direction. We then probed the stacking properties in the nth layer by projecting the particle positions onto the surface. Figure 1 depicts the honeycomblike cells A, B, and C which correspond to the three stacking possibilities that the projection can fall into. Hence one obtains the averaged probabilities $\{p_n^{(A)}, p_n^{(B)}, p_n^{(C)}\}$ for a particle in the nth layer to be projected into a honeycomb of type A, B, or C. The stacking order parameter Ψ_n is now defined as the difference between the two largest numbers of the set $\{p_n^{(A)}, p_n^{(B)}, p_n^{(C)}\}$. For a fluid near a nonstructured wall, all stacking probabilities are equal, hence Ψ_n vanishes. For the first layer of a structured wall, an inhomogeneous liquid has $p_1^{(A)} < p_1^{(B)}$, as it is unlikely for a particle to sit on top of the fixed wall sphere. Furthermore, due to symmetry, $p_1^{(B)} = p_1^{(C)}$; therefore, Ψ_1 vanishes again. A freezing transition in the nth layer is indicated when $\Psi_n > 0$, corresponding to a broken *discrete* symmetry between the two stacking possibilities. Finally, in a perfect (fcc) solid, $\Psi_n = 1$ [13].

The order parameter Ψ_n is shown versus the reduced bulk pressure in Fig. 2 for a triangular pattern. Bulk freezing occurs for $P_c^* = 11.64$, as indicated by the dashed line. As P_c^* is approached from below, there is already a sudden jump in Ψ_1 at $P^* \approx 8.2$, signaling surface freezing in the first layer. Then there is an infinite cascade of subsequent surface freezing transitions in the following layers as the bulk pressure is further increased. We show the first four transitions in Fig. 2. This leads to complete wetting of the substrate by the crystal and is in striking contrast to the continuous growth of sedimentation profiles in hard sphere systems [14]. We have systematically studied these transitions as a function of system size. If the reduced surface area $A^* = L_xL_y/\sigma^2$ of the simulation box is enhanced, the reduced transition pressures P_n^* saturate as depicted in the inset of Fig. 2, proving that our results are beyond finite size corrections. Furthermore, the sharpness of the jumps in Ψ_n versus P^* as indicated by the symbol size in the inset of Fig. 2 scale roughly with $1/\sqrt{A^*}$. This leads to the conclusion that the surface freezing transition is first order. Comparing our data to that of a nonstructured wall [15], there are both qualitative and quantitative differences. First, the nature of the surface freezing transition is different. In our case the lateral translational symmetry is already broken so that first order phase transitions are less obvious. However, the broken discrete stacking symmetry is the key quantity characterizing the transition. Second, the actual numbers for the onset of surface freezing are quite different. While it occurs at a pressure of 3% below P_c^* for a nonstructured wall, it already starts 1 order of magnitude earlier, that is, at 29% below P_c^* in our case.

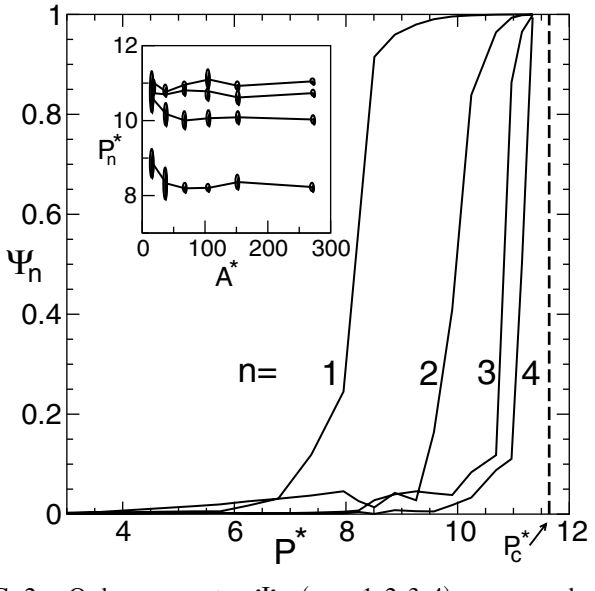

FIG. 2. Order parameter Ψ_n ($n = 1, 2, 3, 4$) versus reduced pressure P^* for a triangular wall pattern with P_c^* indicating the coexistence pressure of the bulk system. The system size is $L_z/\sigma = 45$ and $A^* = 106$. The inset shows the transition pressures P_n^* for $n = 1, 2, 3, 4$ from bottom to top versus the reduced area A^*.

This strikingly demonstrates the decisive role of the substrate pattern which favors the solid phase. For a rhombic pattern we find incomplete wetting by rhombic crystalline sheets proceeding via a finite number of layering transitions. Explicit results are discussed later.

Let us now describe a phenomenological theory for wetting by a crystalline layer. We start from the excess grand canonical free energy Σ per unit area with regard to a nonwetting situation and discuss this quantity if a crystalline sheet of thickness ℓ is present, including contributions from thermodynamics and elasticity theory. The thermodynamical contribution for a wetting layer of thickness ℓ near coexistence, i.e., if $\Delta P = P_c - P > 0$ is small, reads [1]

$$\Sigma_0(\ell) = \gamma_{ws} + \gamma_{sf} - \gamma_{wf} + \alpha \Delta P \ell + \gamma_0 \exp(-\ell/\ell_0) \, . \quad (1)$$

The important ingredients here are the three interfacial free energies, extrapolated to coexistence, between the patterned wall and the solid (γ_{ws}), the patterned wall and the fluid (γ_{wf}), and the bulk solid and fluid (γ_{sf}). $\alpha = (\eta_s - \eta_f)/\eta_f = 0.103$ is the relative density jump across bulk freezing. For large widths ℓ, as we are dealing with short-ranged interparticle interactions, the effective repulsion between the wall-solid and solid-fluid interface decays exponentially, involving a correlation length ℓ_0 in the solid and an amplitude γ_0, which in general will depend on the wall pattern [1]. There is a further free energy penalty $\Sigma_1(\ell)$, if the crystalline sheet is distorted with respect to the coexisting bulk crystal [16]. As motivated by our simulations, the crystal is assumed to be distorted only in lateral directions according to the surface pattern but undistorted in the z direction. Linear elastic theory applied to a wetting layer then yields $\Sigma_1(\ell) = \beta \epsilon^2 \ell$ for small ϵ, where β can be expressed in terms of the elastic constants of the crystal. In the case of a rhombic pattern, $\beta = (C_{11} - C_{12})/2 = 24.43 k_B T/\sigma^3$ for a hard sphere crystal at coexistence [17]. We further assume that γ_0 and ℓ_0 are not affected by the small distortion ϵ. Minimizing $\Sigma_0 + \Sigma_1$ with respect to ℓ yields the realized width as a function of ΔP and ϵ. Note that the phenomenological approach does not predict whether complete wetting occurs as it does not fix the sign of $\gamma_{ws} + \gamma_{sf} - \gamma_{wf}$. Also, since a coarse-grained description is used, there is no discrimination between continuous growth and a cascade of layering transitions. However, once the assumptions of complete wetting are satisfied, the theory predicts quite general asymptotic relations which no longer depend on the interfacial free energies γ_{ws}, γ_{sf}, and γ_{wf}: (i) For vanishing ϵ, the thickness ℓ diverges logarithmically with ΔP, $\ell = -\ell_0 \ln(\ell_0 \alpha \Delta P/\gamma_0)$. (ii) For $\epsilon \neq 0$, there is always incomplete wetting, and the *maximal* thickness which is achieved at $\Delta P = 0$ varies logarithmically with ϵ, $\ell = -\ell_0 \ln(\beta \ell_0 \epsilon^2/\gamma_0)$.

In the insets of Fig. 3 we have tested these two relations against our simulation data using log-linear plots. Good agreement is found for relation (i) as shown in inset 3(a). By fitting a line to our data, we extract actual numbers for the correlation length $\ell_0 = 1.66\sigma$ and the amplitude $\gamma_0 = 0.89 k_B T/\sigma^2$. By using these parameters, relation (ii) is also confirmed [see inset 3(b)]. However, the uncertainty of the data is large since the measured thickness of the layer is necessarily a multiple of the layer spacing $a_z = \sqrt{2/3} a_\triangle$ in the z direction. Note that the solid line in inset 3(b) involves no fit parameters as these are fixed by the fit of inset 3(a).

Furthermore, the layering transition of the nth layer can be estimated by the theory to occur when

$$\alpha \Delta P = \frac{\gamma_0}{\ell_0} \exp(-n a_z/\ell_0) - \beta \epsilon^2. \quad (2)$$

In the plane spanned by ΔP and ϵ^2, the transition lines are predicted to be linear. In fact, as shown in Fig. 3, most of our computer simulation data for the layering transitions fall upon straight lines. We emphasize that the slope does not involve any fit parameter; therefore, quantitative agreement between theory and simulation is obtained within the error bars of the simulation data. However, there are deviations for large strains which we attribute to anharmonic elasticity. In fact, when $\epsilon^2 \to 0.021$, the cost in free energy due to the lateral distortion diverges because then two wall spheres touch. This is not accounted for in the theory.

A further notable fact drawn from Fig. 3 is that there is no surface freezing at all if ϵ exceeds a critical value

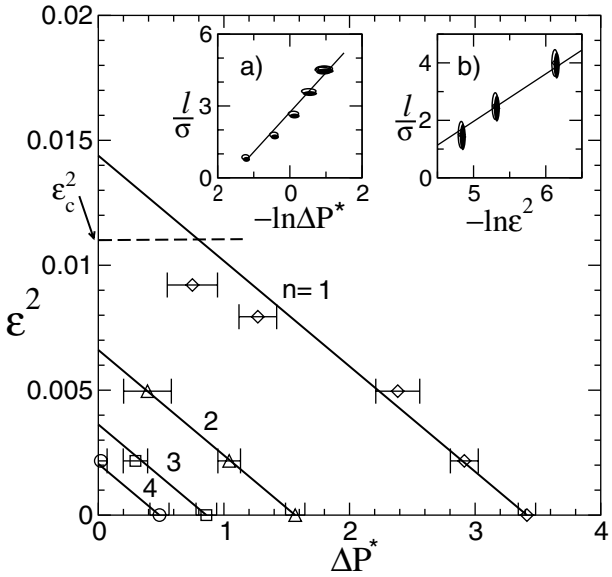

FIG. 3. Location of the first four layering transitions in the plane spanned by ΔP^* and ϵ^2. The symbols represent simulation data with their statistical error. The straight lines are the theoretical predictions. The simulation result for ϵ_c^2 is indicated by the dashed line. Inset (a) shows the thickness ℓ versus $-\ln\Delta P^*$. The straight line here is the best linear fit. Inset (b) shows the maximal thickness ℓ versus $-\ln\epsilon^2$. The straight line is the theoretical prediction. The symbols represent simulation data with the size of the symbols marking the error.

ϵ_c. The theory predicts $\epsilon_c^2 = 0.014$ while the simulations yield a smaller value, $\epsilon_c^2 = 0.011 \pm 0.001$, due to the anharmonic elastic free energy. For $\epsilon > \epsilon_c$ the large free energy cost of elastic distortion prevents the system from surface freezing. The actual situation is a strongly inhomogeneous fluid reflecting the surface pattern which remains stable up to the bulk freezing point.

In conclusion, the structure of a substrate pattern influences profoundly the scenario of surface freezing. First, the onset of surface freezing can be significantly shifted away from coexistence by using a pattern that favors the crystal, as the triangular pattern in our study shows. Second, new surface phases, which are unstable as bulk phases, can be generated by a suitable pattern leading to incomplete freezing at coexistence, as demonstrated for the rhombic pattern in our study. Third, surface freezing can be completely suppressed if the pattern is unfavorable for any solid. The second and third effects were accounted for in a simple phenomenological theory which involves bulk and surface thermodynamics together with elasticity theory of the solid. The corresponding scaling laws were quantitatively confirmed by our simulation data. Our simulation results may serve as benchmark data to test the recently developed density functional theories of hard sphere freezing [18] in inhomogeneous situations. Furthermore, our approach can directly be applied to triple point wetting and to chemically patterned wall structures. As an outlook, we remark that the creation of unstable phases by a surface pattern can be used to prepare "exotic" structures such as quasicrystalline sheets on a suitably patterned template. Future work should focus on the role of crystal defects induced by substrate patterns, which were neglected in our approach and on transitions from commensurate to incommensurate in-plane lattices.

We thank M. Schmidt, R. Evans, and M. Dijkstra for helpful discussions. This work was supported by the Deutsche Forschungsgemeinschaft within project LO 418/5 and by the DAAD Foundation within the ARC Program.

[1] S. Dietrich, in *Phase Transitions and Critical Phenomena,* edited by C. Domb and J. L. Lebowitz (Academic Press, London, 1988), Vol. 12, pp. 1–128.

[2] R. Evans, in *Liquids at Interfaces,* edited by J. Charvolin, J. F. Joanny, and J. Zinn-Justin, Les Houches Session XLVIII (Elsevier, Amsterdam, 1990), p. 1ff.

[3] M. Bernasconi and E. Tosatti, Surf. Sci. Rep. **17**, 363 (1993).

[4] J. C. Earnshaw and C. J. Hughes, Phys. Rev. A **46**, 4494 (1992); X. Z. Wu, E. B. Sirota, S. K. Sinha, B. M. Ocko, and M. Deutsch, Phys. Rev. Lett. **70**, 958 (1993); X. Z. Wu, B. M. Ocko, H. Tang, E. B. Sirota, S. K. Sinha, and M. Deutsch, Phys. Rev. Lett. **75**, 1332 (1995); Y. Hayami and G. Findenegg, Langmuir **13**, 4865 (1997); N. Maeda and V. V. Yaminsky, Phys. Rev. Lett. **84**, 698 (2000).

[5] O. Gang, B. M. Ocko, X. Z. Wu, E. B. Sirota, and M. Deutsch, Phys. Rev. Lett. **80**, 1264 (1998); Phys. Rev. Lett. **82**, 588 (1999).

[6] A. Weinstein and S. A. Safran, Phys. Rev. E **53**, R45 (1996); A. V. Tkachenko and Y. Rabin, Phys. Rev. E **55**, 778 (1997); P. K. Mukherjee and M. Deutsch, Phys. Rev. E **61**, 637 (2000).

[7] P. Smith, R. M. Lynden-Bell, J. C. Earnshaw, and W. Smith, Mol. Phys. **96**, 249 (1999).

[8] P. Lenz and R. Lipowsky, Phys. Rev. Lett. **80**, 1920 (1998); C. Bauer and S. Dietrich, Phys. Rev. E **60**, 6919 (1999); L. J. Frink and A. G. Salingers, J. Chem. Phys. **110**, 5969 (1999).

[9] S. Herminghaus *et al.,* J. Phys. Condens. Matter **12**, A8 (2000).

[10] F. H. Ree and W. G. Hoover, J. Chem. Phys. **46**, 4181 (1967).

[11] A. K. Arora and R. Rajagopalan, Curr. Opin. Colloid Interface Sci. **2**, 391 (1997); A. van Blaaderen, R. Ruel, and P. Wiltzius, Nature (London) **385**, 321 (1997); F. Burmeister, C. Schäfle, T. Matthes, M. Bohmisch, J. Boneberg, and P. Leiderer, Langmuir **13**, 2983 (1997); C. Mio and D. W. M. Marr, Langmuir **15**, 8565 (1999).

[12] W. J. Huisman *et al.,* Nature (London) **390**, 379 (1997).

[13] We have also calculated the bond orientational order parameter ψ_6 [see, e.g., A. Jaster, Physica (Amsterdam) **277A**, 106 (2000)]. Although similar transition points are extractable from the distribution of ψ_6, the statistical error is much larger because ψ_6 is sensitive to rotational symmetry, which in our case is already broken by the wall.

[14] T. Biben, R. Ohnesorge, and H. Löwen, Europhys. Lett. **28**, 665 (1994).

[15] D. J. Courtemanche and F. van Swol, Phys. Rev. Lett. **69**, 2078 (1992); D. J. Courtemanche, T. A. Pasmore, and F. van Swol, Mol. Phys. **80**, 861 (1993).

[16] F. T. Gittes and M. Schick, Phys. Rev. B **30**, 209 (1984).

[17] D. Frenkel and A. J. C. Ladd, Phys. Rev. Lett. **59**, 1169 (1987).

[18] Y. Rosenfeld, Mol. Phys. **94**, 929 (1998).